

Energetics of twisted elastic filament pairs

Julien Chopin,¹ Animesh Biswas² and Arshad Kudrolli²

¹ *Instituto de Física, Universidade Federal da Bahia, Salvador-BA 40170-115, Brazil*

² *Department of Physics, Clark University, Worcester, Massachusetts 01610, USA*

(Dated: February 20, 2024)

We investigate the elastic energy stored in a filament pair as a function of applied twist by measuring torque under prescribed end-to-end separation conditions. We show that the torque increases rapidly to a peak with applied twist when the filaments are initially separate, then decreases to a minimum as the filaments cross and come into contact. The torque then increases again while the filaments form a double helix with increasing twist. A nonlinear elasto-geometric model that combines the effect of geometrical nonlinearities with large stretching and self-twist is shown to capture the evolution of the helical geometry, the torque profile, and the stored energy with twist. We find that a large fraction of the total energy is stored in stretching the filaments, which increases with separation distance and applied tension. We find that only a small fraction of energy is stored in the form of bending energy, and that the contribution due to contact energy is negligible. Further, we provide analytical formulas for the torque observed as a function of the applied twist and the inverse relation of the observed angle for a given applied torque in the Hookean limit. Our study highlights the consequences of stretchability on filament twisting which is a fundamental topological transformation relevant to making ropes, tying shoelaces, actuating robots, and the physical properties of entangled polymers.

I. INTRODUCTION

Twisting and braiding filaments are relevant to making ropes, tangling, and are an important construct in bio-materials [1–8]. It is an important step in tying a knot, where the contact structure for filaments meeting even at 90° can be quite complex [9]. A common element in windup toys (see Fig. 1(a)), elastomeric filaments are being developed towards applications in novel energy storage and rapid mechanical actuation [10–13]. The twist of a single filament itself can be quite subtle [14]. While the filament deforms uniformly when twist is applied at its ends about its central axis, a helical instability occurs above a critical twist depending on the applied tension, which causes the central line of the filament to follow a helical path about the central axis [15, 16]. The pitch cannot be less than the diameter of the filament limiting the phase space of possible winding angles that a filament can have [17, 18]. Although polymer filaments are typically hyperelastic, their analysis has often treated them as being inextensible [19–21]. The effective radius and contraction of filament bundles have been measured as a function of applied twist and shown to deviate from models based on volume conservation [22]. Braiding and torque of extended and twisted DNA pairs was investigated by Charvin, et al. [23] with experiments and models which mainly considered bending energy.

Here, we investigate the energy stored in a pair of elastic filaments by measuring and analyzing the torque as a function of applied twist with an elasto-geometric model. This system is not only important in its own right, but also forms a basis to understand the topology and energetics of multi-filament bundles where geometric frustration leads to further complexity in arriving at their configurations with twist [21, 24]. A priori one may expect energy contributions from bending, stretching, and twist-

ing of each filament, and the filament-filament contact. We consider a regime where the material deformations themselves can be considered as linear or neo-Hookean, but where the geometry of the configurations leads to a complex response. We show that energy is essentially stored in twisting and stretching the filaments which vary in relative magnitude depending on the system geometry and applied twist. The contribution of bending and inter-filament contact are found to be negligible over the observed twist angles.

In the following, we first discuss the experimental measurements of the geometry and the torque encountered as a function of the applied twist with elastic filament-pairs in Section II. Then, we develop an elasto-geometric model by considering the energy stored assuming neo-Hookean response under large deformations and compare it with the measured data in Section III, and calculate the energy stored within stretch, bend, twist and contact components in Section IV. Before concluding, we provide analytical formulas in the limit of Hookean response, and discuss the twist angle reached under prescribed torque conditions in Section V.

II. EXPERIMENTS

We consider two elastic filaments with radius R_0 (diameter $D_0 = 2R_0$) and relaxed length L_0 , that are initially parallel and separated by a distance W and clamped at their ends as shown in Fig. 1(b). The filaments can be also pre-stretched by a distance ΔL , resulting in a length $L = L_0 + \Delta L$. The filaments are twisted through end-to-end angle θ about the central axis which parallels the initial orientation of the filaments. The filaments are composed of silicone (USA Industrials) and have a circular cross section of radius $R_0 = 1.27$ mm. We

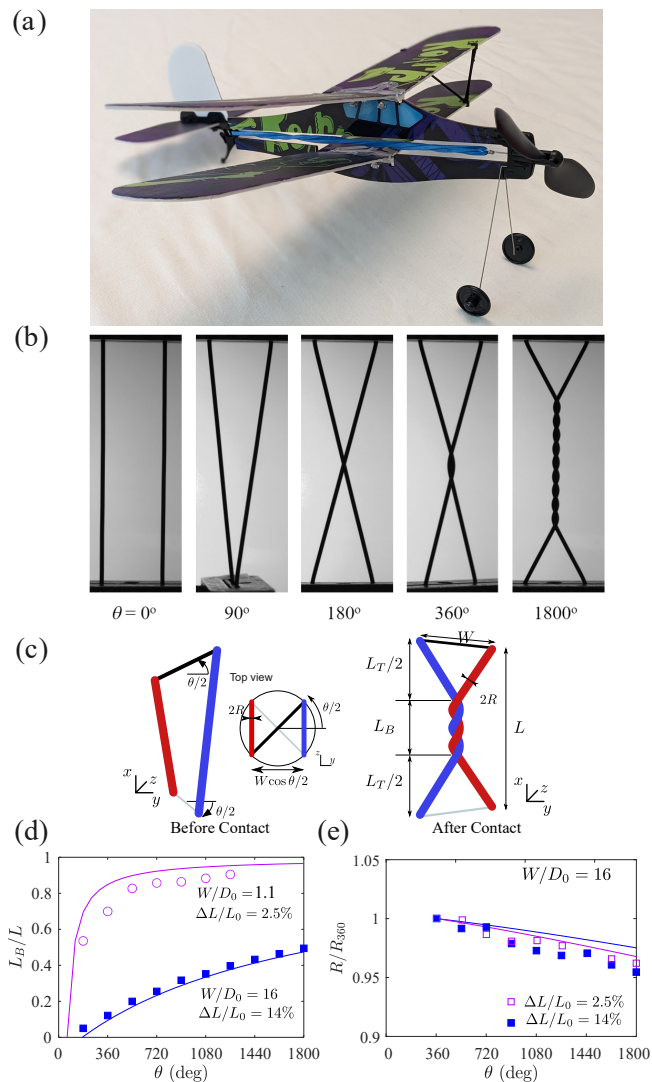


FIG. 1. (a) A rubber band airplane powered by elastic energy. (b) Images of the filaments twisted about the central axis while clamped at a fixed distance $L/L_0 = 1.14$ and $W/D_0 = 16$ apart. (c) Schematic of the filament geometry before the filaments come in contact and after contact when a helical bundle forms at the center. (d) The measured evolution of the bundle size L_B/L for various W and comparison with Eq. (20). (e) The bundle radius as a function of twist normalized by the radius R_{360} at $\theta = 360^\circ$ and Eq. (2), where λ is obtained using the elasto-geometric model.

perform measurements of torque with a Mark-10 MR50-10Z torque sensor fixed to the top clamp. The bottom clamp is rotated through a prescribed angle θ with a computer controlled microstepper motor, and images are taken with a 9.6 megapixel Pixelink PL-D729MU camera while θ is incremented in 1° steps.

Figure 1(b) shows a sequence of images as the filaments are twisted around each other 5 times when $L = 17.2$ cm and $W = 4$ cm. As shown schematically in Fig. 1(c), the filaments can be represented as straight lines before contact at twist angle θ_c if the curvature due to bending

at the clamps is negligible, and then as a double helix connected to essentially straight filament segments after contact. We measure and plot the helical bundle length L_B in Fig. 1(d), and the helical bundle radius R normalized by the radius R_{360} after one full twist corresponding to $\theta = 360^\circ$ in Fig. 1(e). (As a consequence of geometry, this radius can be seen to be the same as the radius of the filament if the contact deformation is negligible.) We observe that the double helix grows in length while its radius decreases slowly with increasing θ depending on W .

These changes in the geometry can be seen to have significant effects on the torque required to twist the filaments. Figure 2(a) shows the torque M measured as a function of θ corresponding to $L/W = 4.2$ and $W/D_0 = 16$. We observe that the torque increases rapidly before decreasing to a minimum when the filaments come in contact, and then rises again. The appearance of a peak may seem surprising, but it has been seen previously in twisted DNA [23]. A similar feature has been also noted in a twisted sheet, besides further non-monotonous behavior at higher twists due to shape transformations [25]. When $W \approx D_0$, the peak is absent and a monotonic increasing torque is observed (see Inset to Fig. 2(a)). As illustrated in Fig. 2(b), decreasing pre-stretch is observed to lead to an overall decrease in M , but the peak is present even when $L \simeq L_0$, and the overall variation of M with θ is similar for all the cases.

The elastic energy stored in the filaments can be obtained by integrating the torque over the twist angle, i.e. $E_{tot} = \sum_0^\theta M \Delta\theta$, where $\Delta\theta$ corresponds to 1° in our experiments. The corresponding data are plotted in Fig. 2(c) and show that E_{tot} increases monotonically with θ . The energy is a smooth function without kink or discontinuity at the point of contact as it is obtained by integrating the torque which is a continuous function of the twist angle. Further, it can be observed that the energy increases rapidly with increasing W before filaments come in contact, and then increases more slowly after they cross. Thus, the total stored energy can be increased significantly by simply separating the filaments for the same amount of elastic material.

III. ELASTO-GEOMETRIC MODEL

We now develop a model which can capture the geometry of the twisted filament, the torque, and the stored elastic energy as a function of twist angle. An established method to understand such problems is to consider the elastic energy stored in the system, and consider its variation with appropriate stretch parameter to obtain the force or torque required as a function of applied boundary conditions [26].

Figure 3(a) shows the applied nominal stress $\sigma_N = F/S_0$, where F is the applied longitudinal force and $S_0 = (\pi/4)D_0^2$, versus measured stretch $\lambda = L/L_0$ along the length of the filaments. We observe that the stress

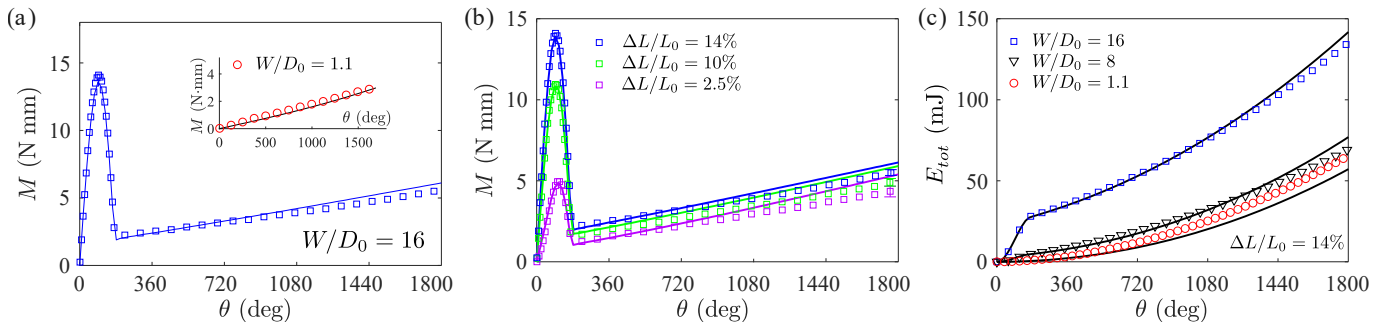


FIG. 2. (a) The measured (marker) torque versus twist angle. Comparison with Neo-Hookean model (thin blue/gray line). Inset: The measured torque when $W = 2R_0$ compared with model. (b) Measured and calculated torque versus twist angle for 2-filament twist for $W = 4$ cm for various pre-stretch conditions L/L_0 . The peak before filaments come in contact increases with L . The calculated torque using stretching, twist and bending energy assuming Neo-Hookean model with no fit parameters. Good overall agreement is observed. The measurement errors are indicated by bars on the last set of markers. (c) The measured (markers) and corresponding calculated (lines with corresponding color/shade) energy as a function of twist for various W . The stored energy increases with separation distance.

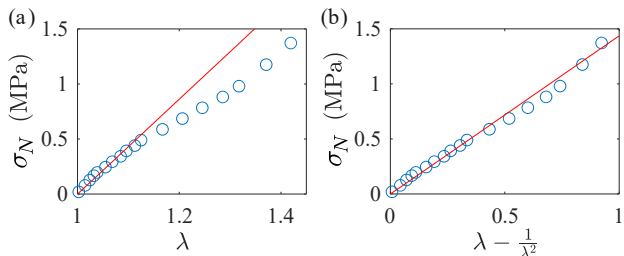


FIG. 3. (a) Nominal stress σ_N as a function of λ is sublinear for large enough extensions. (b) σ_N scales linearly as a function of $\lambda - \frac{1}{\lambda^2}$, where $\lambda = L/L_0$ since $\mathcal{L} = L$ as the filaments are not twisted during these measurements. The linear fit confirms the neo-Hookean nature of the filament, and yields shear modulus $\mu = 1.43 \pm 0.1$ MPa.

increases linearly initially, but then becomes weakly non-linear. This is a hallmark of a neo-Hookean response. Then, the strain-energy function [27]:

$$\mathcal{W} = \frac{1}{2}\mu(\lambda_1^2 + \lambda_2^2 + \lambda_3^2 - 3), \quad \lambda_1\lambda_2\lambda_3 = 1, \quad (1)$$

where λ_i are the principal stretches and μ is the shear modulus. For uniaxial stretching, $\lambda_1 = \lambda$ along the filament axis, $\lambda_2 = \lambda_3 = 1/\sqrt{\lambda}$. Hence, the radius R of a stretched filament is reduced due to volume conservation and is given by:

$$R = R_0/\sqrt{\lambda}. \quad (2)$$

Accordingly, for a uniaxially stretched filament, the nominal stress σ_N is given by [27],

$$\sigma_N = \mu \left(\lambda - \frac{1}{\lambda^2} \right). \quad (3)$$

In Fig. 3(b), we find that the data agrees with the neo-Hookean model with $\mu = 1.43 \pm 0.1$ MPa over the typical stretches experienced in our system.

We parameterize the kinematics of the filament pairs to obtain the stretch as a function of twist. Before contact ($\theta < \theta_c$), the shapes of the filaments are modeled by straight lines connecting the top and bottom clamps (see Fig. 1(c)). One may expect a region of order R_0 from the clamp to be curved, but we neglect this as being relatively small, as can be noted from Fig. 1(b). After contact ($\theta \geq \theta_c$), as seen from Fig. 1(b), the filament geometry can be divided into a central helicoidal section of length L_B , and two triangular sections next to the clamps of height L_T in total, with $L = L_B + L_T$. The central shape where the filaments are in enduring contact is modeled as a double helix of length L_B , radius R , and helix angle β . Therefore, the curvature in the helix is given by [28]:

$$\kappa = \frac{1}{R} \frac{\tan^2 \beta}{1 + \tan^2 \beta}, \quad (4)$$

with $\tan \beta = R(\theta - \theta_c)/L_B = \Delta q/l_B$, $\Delta q = R(\theta - \theta_c)/L$ and $l_B = L_B/L$. The torsion τ is assumed to be homogeneous along the entire filament and given by $\tau = \theta/\mathcal{L}$ where \mathcal{L} is the curvilinear length of a filament.

As can be seen from the top view in Fig. 1(c), the distance between the filaments in the yz -plane is $W \cos \theta/2$. Thus, contact occurs when $W \cos \theta_c/2 = 2R$, yielding

$$\theta_c = 2 \arccos \left(\frac{2R}{W} \right) \quad (5)$$

for $R/W < 1/2$. If the filaments are initially close to each other, i.e. $W \approx D_0$, θ_c varies rapidly with pre-stretch and is given by $\theta_c \approx 2\sqrt{\lambda - 1}$.

After parametrizing the shape, we can evaluate the filament deformation using the longitudinal stretch factor

$$\lambda = \mathcal{L}/L_0. \quad (6)$$

Before contact, as the filaments are modeled by straight lines, \mathcal{L} is given as the distance between the top

and bottom clamps, hence:

$$\lambda = \lambda_0 \sqrt{1 + \left(\frac{W}{L} \sin \frac{\theta}{2}\right)^2}, \quad \theta < \theta_c, \quad (7)$$

where $\lambda_0 = L/L_0$ is the stretch factor before twist where $\theta = 0$.

After contact, the inserted twist in the helix is $\Delta\theta = \theta - \theta_c$ and the arc length of the helix is given by

$$\mathcal{L}_B = L \sqrt{l_B^2 + \Delta q^2}, \quad (8)$$

with $\Delta q = \Delta\theta R/L$, and $l_B = L_B/L$. Outside the helical region, the filaments are not in contact and are assumed to be straight lines. The filaments form two triangles of height $L_T/2 = (L - L_B)/2$ each and base size W in that region. We can calculate the triangle side length \mathcal{L}_T by evaluating the distance between the clamped end of one of the filaments, say the right one, and the point at which the filament enters into the helix at $(L_B/2, R \cos(\Delta\theta/2), R \sin(\Delta\theta/2))$. Thus, $(\mathcal{L}_T/2)^2 = (L_T/2)^2 + (W/2 \cos(\theta/2) - R \cos(\Delta\theta/2))^2 + (W/2 \sin(\theta/2) - R \sin(\Delta\theta/2))^2$. Using Eq. (5) and trigonometric identities, we have

$$\mathcal{L}_T = L \sqrt{l_T^2 + \Delta w^2}, \quad (9)$$

where $l_T = L_T/L$, and $\Delta w = \sqrt{W^2 - 4R^2}/L$.

From the total arc length of the filament given by $\mathcal{L} = \mathcal{L}_B + \mathcal{L}_T$ and Eq. (6), we obtain

$$\lambda = \lambda_0 \sqrt{l_T^2 + \Delta w^2} + \lambda_0 \sqrt{l_B^2 + \Delta q^2}, \quad \theta \geq \theta_c. \quad (10)$$

Thus, λ is completely known once l_T and l_B are determined. Since $1 = l_B + l_T$, we only need to determine, say, l_B which can be found by minimizing the total elastic energy E_{tot} .

In the two-filament system, the total energy can be written as

$$E_{tot} = E_t + E_s + E_b + E_c, \quad (11)$$

where E_t is the energy associated with twisting the filaments about their axis, E_s is the energy associated with stretching the filaments, E_b is the energy associated with bending the filaments into the helical shapes that they adopt with twist, and E_c is the energy due to filaments contact contractions. The twist energy of the two filaments is given by [29],

$$E_t = \frac{1}{2} \mu V \frac{q_0^2}{\lambda}, \quad (12)$$

where $q_0 = R_0\theta/L_0$. $V = \pi R_0^2 L_0$ is the volume in the reference (zero-load) configuration. The twist-induced stretching energy is given by [30]

$$E_s = \mu V \left(\lambda^2 + \frac{2}{\lambda} - 3 \right) - E_s^o, \quad (13)$$

where $E_s^o = \mu V \left(\lambda_0^2 + \frac{2}{\lambda_0} - 3 \right)$ is the stretching energy after pre-stretching. With this definition, the total energy is zero after pre-stretching, consistent with our definition $E_{tot} = \sum_0^\theta M \Delta\theta$. The bending energy is given by [31], $E_b = B/2 (\mathcal{L}_B/\lambda) \kappa^2$, where $B = 3/4 \mu \pi R_0^4 = 3/4 \mu V R_0^2/L_0$ is the bending rigidity. Thus,

$$E_b = \frac{3}{8} \mu V \lambda (\kappa R)^2 \frac{\mathcal{L}_B}{\mathcal{L}}, \quad (14)$$

where we use the fact that $R_0^2/L_0 = \lambda^2 R^2/\mathcal{L}$. The λ -dependence of R is given by Eq. (2). The inter-filament contact energy E_c can be estimated by assuming the curvature is small enough that the curved contact can be considered as a straight line. The Hertz contact energy of two parallel cylinders pressed against each other, forming a contact over a length \mathcal{L}_B , is given by $E_c = \pi/2 \mu (\delta R)^2 \mathcal{L}_B$ [21, 32], where δR is the indentation of the two filaments upon self-contact. Therefore, we have:

$$E_c = \frac{1}{2} \mu V \left(\frac{\delta R}{R} \right)^2 \frac{\mathcal{L}_B}{\mathcal{L}}. \quad (15)$$

To obtain δR , we consider a force equilibrium between the normal inward force $(\sigma_N \pi R_0^2) \kappa \mathcal{L}_B = (\sigma_N V) \kappa \lambda (\mathcal{L}_B/\mathcal{L})$ and the Hertz resisting force [32], $dE_c/d(\delta R) = \mu V (\delta R/R^2) (\mathcal{L}_B/\mathcal{L})$, which gives:

$$\frac{\delta R}{R} \approx \frac{\sigma_N \lambda}{\mu} \kappa R. \quad (16)$$

After substituting in Eq. (15), this yields

$$E_c = \frac{1}{2} \mu V \left(\lambda^2 - \frac{1}{\lambda} \right)^2 (\kappa R)^2 \frac{\mathcal{L}_B}{\mathcal{L}}, \quad (17)$$

where we use $\sigma_N \lambda = \mu (\lambda^2 - 1/\lambda)$, following Eq. (3).

Then, we find numerically the bundle length l_B which minimizes E_{tot} and compare its evolution as a function of θ for various W with experiments in Fig. 1(d). We obtain good agreement without fitting parameters. Further, R as a function of θ is calculated using Eq. (2) and found to also be in overall good agreement with the measured values (see Fig. 1(e)). Thus, the geometry of the twisted filaments can be captured by the elasto-geometric model by simply using energy minimization.

Having found l_B , we evaluate E_{tot} , and plot it as a function of θ for the three different W in Fig. 2(c). We observe that it follows the measured values without any fitting parameters within experimental error. Finally, we obtain the torque profile by numerical differentiation since $M = \partial E_{tot}/\partial\theta$ to directly compare with the measurements. Figure 2(a) shows the comparison for $W = 4$ cm and for $W = D_0$ in the Inset to Fig. 2(a), where quantitative agreement can be observed in each case without fitting parameters. Thus, we have a fully tested model of the geometry, torque and elastic energy stored in twisted two-filament pairs with neo-Hookean material properties.

IV. ENERGY COMPONENTS

We examine the various energy components to understand their relative contributions due to geometry and pre-stress. Figure 4(a-c) shows E_{tot} for the three different W . We observe that the contribution of twisting energy to total energy is larger than stretching when the filaments are close together, but stretching makes an increasingly greater contribution with increasing W . Furthermore, it can be noted that bending contributes a little to the total energy, and that the contribution of contact energy is in fact smaller than the line width, so we have not plotted it.

To tease out the twist and stretching energy contributions to the total energy further, we plot the ratio E_t/E_{tot} and E_s/E_{tot} in Fig. 5 for the various W and $\Delta L/L_0$. We observe that a large fraction of the total energy is stored in the twist mode when pre-stretch $\Delta L/L_0$ is small, but an increasing fraction is in the stretch mode as the filaments are stretched about the axis of rotation. In other words, increasing W and ΔL for the same length of filament L_0 leads to increasing E_{tot} , with increasing fraction stored as stretching energy. This suggests a maximization strategy for total stored energy per unit filament length, by increasing pre-stretch and separation distance between twisted filaments one increase store energy for the same amount of material and number of twist turns.

V. ANALYTICAL FORMULAS FOR ENERGY AND TORQUE

We next examine some analytical limits of our elastogeometric model in order to provide formulas of energy and torque in the case of twisted elastic filaments.

A. Filament pairs in contact in the Hookean limit

When the two filaments are initially in contact, the calculation of λ is straightforward as they are modeled by stretched helices, yielding $\lambda = \lambda_0 \sqrt{1 + (R\theta/L)^2}$ which corresponds to Eq. (10) with $L = L_B$ and $\Delta w = l_T = 0$. In the Hookean limit, for $\Delta L/L_0 \sim (R_0/L_0)^2 \ll 1$, we have $\lambda \approx \lambda_0 + \frac{1}{2} (R_0/L_0)^2 \theta^2$ and $\lambda_0 \approx 1 + \Delta L/L_0$. Thus,

$$\frac{M}{\mu V} = \left(\frac{R_0}{L_0}\right)^2 \left(1 + 6\frac{\Delta L}{L_0}\right) \theta. \quad (18)$$

Therefore, the stretching of the filament introduces an additional term in the torque which scales in the Hookean limit as $(R_0/L_0)^2(\Delta L/L_0)$.

We compare the torques obtained using these analytical calculations assuming Hookean-response and those assuming neo-Hookean response in Fig. 6(a). We observe that these calculations agree for sufficiently small $\Delta L/L_0$, but deviations are observed as $\Delta L/L_0$ is increased to 20%.

B. Filament pairs with separation

1. Before Contact

Since the filaments are described by straight lines, $\kappa = 0$, and thus $E_B = E_c = 0$. Thus, a general expression for the torque can be obtained using the chain rule $M = \frac{\partial E_{tot}}{\partial \theta} = \frac{\partial E_{tot}}{\partial \lambda} \frac{\partial \lambda}{\partial \theta}$, with $E_{tot} = E_t + E_s$. Then,

$$\frac{M}{\mu V} = \left(1 - \frac{1}{\lambda^3} \left(1 + \frac{1}{4} \left(\frac{R_0}{L_0}\right)^2\right)\right) \frac{\partial \lambda^2}{\partial \theta} + \frac{1}{\lambda} \left(\frac{R_0}{L_0}\right)^2 \theta,$$

Then, using Eq. 7, we have, in the Hookean limit

$$\frac{M}{\mu V} = \frac{3}{2} \left(\frac{W}{L_0}\right)^2 \frac{\Delta L}{L_0} \sin \theta + \left(\frac{R_0}{L_0}\right)^2 \theta. \quad (19)$$

Thus, for $\theta < \theta_c$, the ratio between the stretch and twist contributions is given approximately by the stretch/twist ratio $\mathcal{R} = 6\frac{\Delta L}{L_0} \left(\frac{W}{D_0}\right)^2$. For $W \approx D_0$, twist contribution dominates as $\mathcal{R} \approx 6\Delta L/L_0 \ll 1$ in the Hookean limit and $\frac{M}{\mu V} \approx \left(\frac{R_0}{L_0}\right)^2 \theta$ is pre-stretch independent. For large W (i.e. $W \gg D_0$), the stretch/twist ratio \mathcal{R} depends both on geometry and pre-stretch. When $\frac{\Delta L}{L_0} \ll \left(\frac{D_0}{W}\right)^2 \ll 1$ (or, equivalently, $\mathcal{R} \ll 1$), the torque $\frac{M}{\mu V} \approx \left(\frac{R_0}{L_0}\right)^2 \theta$ is still independent on the pre-stretch. But, for larger pre-stretch $\left(\frac{D_0}{W}\right)^2 \ll \frac{\Delta L}{L_0} \ll 1$ (or, equivalently, $\mathcal{R} \gg 1$), stretch contribution dominates yielding a torque that increases linearly with the pre-stretch and reads $\frac{M}{\mu V} = \frac{3}{2} \left(\frac{W}{L_0}\right)^2 \frac{\Delta L}{L_0} \sin \theta$.

2. After Contact

We can solve the problem of finding the bundle length L_B asymptotically after contact, and show that $\partial E_{tot}/\partial L_B = 0$ reduces to $\partial \lambda/\partial L_B = 0$. Consistent with numerical analysis which finds bending and contact contributions to be small, they are not included. We will check a posteriori that the bending contribution to the total energy is negligible in the limit $L_0 \gg \theta R$. Using Eq. (10), the minimization scheme yields after some algebra:

$$l_B = 1 - l_T = \frac{\Delta q}{\Delta w + \Delta q}. \quad (20)$$

Substituting Eq. (20) in Eq. (10),

$$\lambda = \lambda_0 \sqrt{1 + (\Delta w + \Delta q)^2}. \quad (21)$$

Using Eq. (6), Eq. (8), and Eq. (20), we also have that $\mathcal{L}_B/\mathcal{L} = \sqrt{l_B^2 + \Delta q^2}/\sqrt{1 + (\Delta q + \Delta w)^2} = l_B$. Likewise, we obtain $\mathcal{L}_T/\mathcal{L} = l_T$. Note that θ_c , Δq , and dw

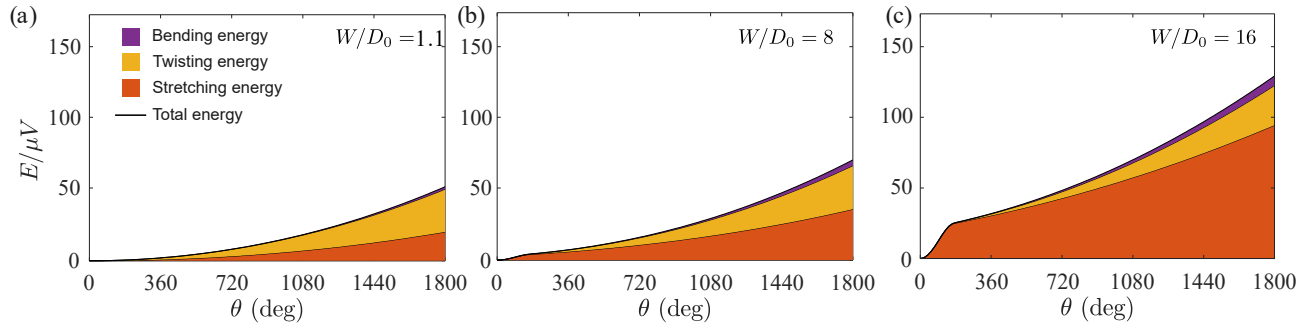


FIG. 4. (a-c) The contribution of twisting, bending, and stretching energies to total stored energy as a function of twist for various W . The contact energy contribution is negligible and thus not plotted. ($\Delta L/L_0 = 0.14$, same as in Fig. 2(c)).

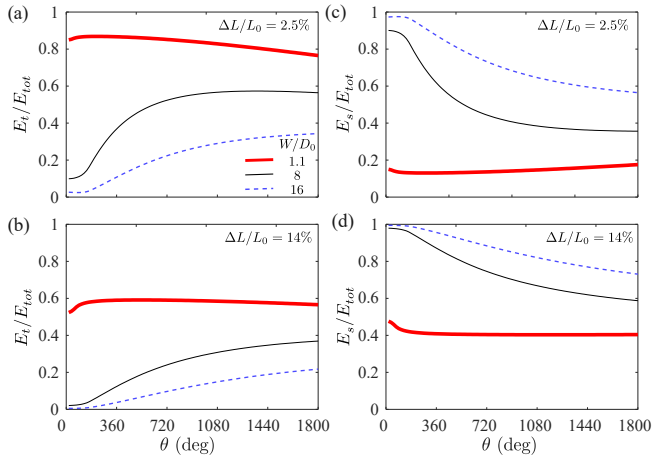


FIG. 5. Energy fraction for various W and λ stored in twist (a,b), and in stretching (c,d). While most of the total energy is in the form of twist at lowest $\Delta L/L_0$ and W , an increasing fraction is stored in stretching the filaments with twist. Energy stored in stretching the filaments dominates as W and $\Delta L/L_0$ are increased.

should depend on λ through R . To obtain a closed form of expression for λ , we take $R \approx R_0/\sqrt{\lambda_0}$. This gives an accurate expression if λ remains close to λ_0 , which occurs when Δw and Δq are small. Now, we evaluate the bending energy to check that it is indeed negligible in the limit $R\theta/L \ll 1$ and $W/L \ll 1$. Using Eqs (4), (14) and (21), we find that $\kappa R \approx (\Delta q + \Delta w)^2$ and $E_b \sim (\Delta q + \Delta w)^3 \Delta q$. Interestingly, we find that the bending energy increases with W because the curvature increase with W overcompensates for the decrease in $\mathcal{L}_B/\mathcal{L} = l_B$ (see Eq. 20). Then, using Eqs. (12) and (13), we find that $E_s \sim (\Delta q + \Delta w)^2$, $E_t \sim q_0^2$, and $E_b \sim (\Delta q + \Delta w)^3 \Delta q \ll E_s, E_t$ when $\Delta q, \Delta w \ll 1$. For five turns and $W = 40$ mm, $\Delta q \approx 1/3$ and $\Delta w \approx 1/5$ are not much smaller than unity which explains why bending energy is predicted to be a fraction of the twisting and stretching energy. Thus, bending energy can be neglected at a small enough twist angle.

Finally, the torque after self-contact is given by substituting in Eq. (21) in Eq. (12) and Eq. (13). Using the

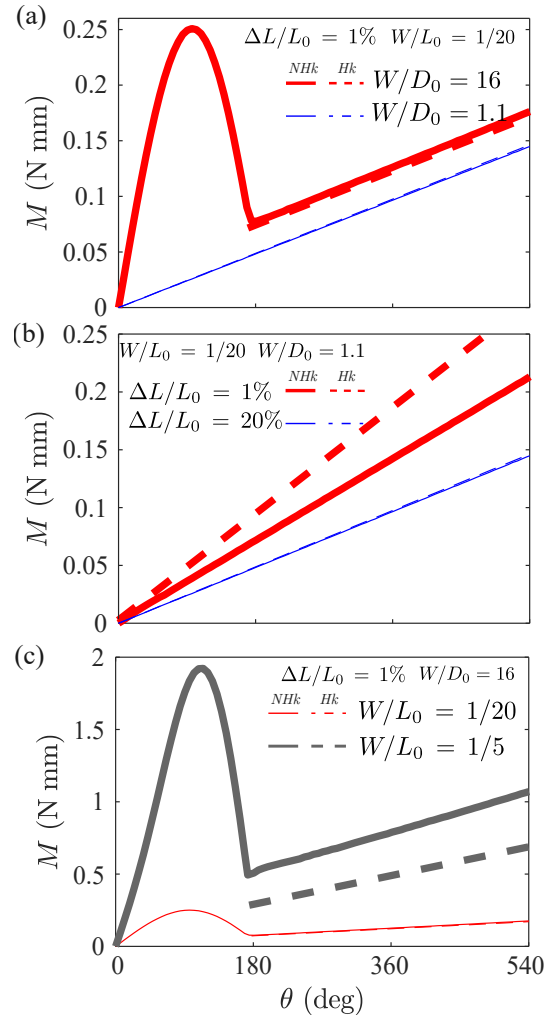


FIG. 6. Torque as a function θ after contact calculated from the Neo-Hookean (NHk) model (solid thick red and thin blue lines) and the Hookean (Hk) limit given by Eq. (22) (dashed thick red and thin blue lines). (a) The Neo-Hookean and Hookean curves agree for small $\Delta L/L_0$. (b,c) The two estimates agree for sufficiently small $\Delta L/L_0$ for small enough L/W (b), but disagree for large $W/L_0 = 1/5$ (c).

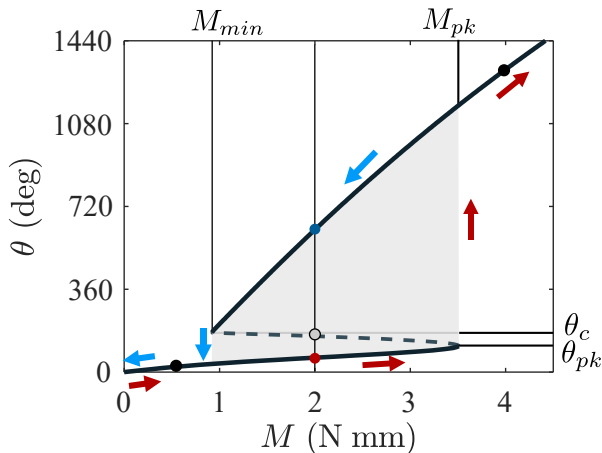


FIG. 7. The twist angle versus torque profile (solid and dashed black lines) under torque prescribed conditions using our elasto-geometric model with $\Delta L/L_0 = 1\%$, and $W/D_0 = 16$. Unlike for twist prescribed experiments, the profile is multi-valued for torque values between the minimum M_{min} and peak value M_{pk} . The multi-valued profile leads to a hysteresis cycle (see gray area and arrows). Vertical lines at M_{min} and M_{pk} corresponds to dynamics jumps from one stable branch to the other. θ_{pk} is the twist angle corresponding to the peak value of the torque.

chain rule as before, we have in the Hookean limit

$$\frac{M}{\mu V} = \left(\frac{R_0}{L_0}\right) \left(6 \frac{\Delta L}{L_0} \Delta w + q_0\right). \quad (22)$$

We compare these asymptotic calculations carried out in the case of Hookean-response with numerical calculations with the full elasto-geometric model in cases where the filaments are separate in Fig. 6(b,c). One can note from Fig. 6(b) that the spacing between the filament $W > 2R_0$ introduces an additional term in the torque, proportional to Δw . This term introduces an offset in the torque independent of θ and scales as $(RW/L_0^2) (\Delta L/L_0)$. Further comparing the two calculations for small $\Delta L/L_0$, we observe deviations for sufficiently large W/L_0 (see Fig. 6(c)). This can be understood from the fact that the filaments are stretched significantly as θ is increased to 180° .

C. Prescribed torque

The analysis which enables us to determine the torque required to twist the filament-pair as a function of angle also allows us to determine the angle reached if a prescribed torque is applied. In Fig. 7, we show the twist angle versus torque obtained from our elasto-geometric model ($\Delta L/L_0 = 1\%$, $W/D_0 = 16$) by inverting the relation $M(\theta)$ numerically. Unlike under the twist prescribed conditions, the profile is multi-valued. We predict two stable branches (solid black line) and one unstable

branch (dashed black line) which corresponds to the decreasing part of the peak in twist angle controlled experiments. Outside this interval, there is only one stable branch. Thus, if the torque is increased quasi-statically from zero, the resulting twist angle increases slowly until $M = M_{pk}$ where the twist angle jumps dynamically to a larger equilibrium value on the stable top branch. Now, decreasing the torque starting from a value larger than M_{pk} , the twist angle decreases until $M = M_{min}$, where the twist angle jumps dynamically to the stable bottom branch. In a torque controlled experiment, we thus have a hysteresis cycle (gray area) which originates from the existence of a non-monotonous torque profile. The hysteretic behavior can be expected to vanish as $W \rightarrow D_0$, i.e. when the torque profile becomes monotonous.

We provide analytic expressions for the twist angle in torque controlled experiments. In case of filaments which are in contact, this corresponds to simply inverting the relation given by Eq. (18), and rewriting θ in terms of M , i.e.

$$\theta = \frac{1}{\mu V} \left(\frac{L_0}{R_0}\right)^2 \left(1 + 6 \frac{\Delta L}{L_0}\right)^{-1} M. \quad (23)$$

However, in the case where filaments are separate, there can be more than one stable angle depending on the applied torque in relation to the peak reached before the filaments come in contact, and the minimum when the filaments first come in contact. This can be easily seen by considering the intersection of horizontal lines corresponding the prescribed torque with M - θ plots shown in Fig. 2(a,b).

Before filaments come in contact, the stable angle can be obtained in general by solving Eq. (19) numerically, but in the case of large pre-stretch (i.e. $(\frac{D_0}{W})^2 \ll \frac{\Delta L}{L_0} \ll 1$), we have,

$$\theta = \sin^{-1} \left(\frac{2}{3} \frac{M}{\mu V} \frac{L_0^3}{\Delta L W^2} \right). \quad (24)$$

After contact, the twist angle that can be reached for a prescribed torque is obtained by inverting Eq. (22), yielding

$$\theta = \frac{M}{\mu V} \left(\frac{L_0}{R_0}\right)^2 - 6 \frac{\Delta L}{L_0} \frac{W}{R_0}, \quad (25)$$

where we use the fact that $\Delta w \approx W/L_0$ for $W \gg D_0$.

Thus, we find that two stable angles are possible for filaments where $W > D_0$ when applied torque is between the torque-minima when filaments come in contact and the peak value encountered before filaments come in contact. The angle reached in practice then depends on the initial conditions. In the case of filaments which are initially untwisted and parallel, θ corresponds to the angle before contact given by Eq. (24). However for initial twist angles corresponding to those greater than when filaments are contact, θ reached corresponds to Eq. (25).

VI. CONCLUSIONS

In summary, we investigated the torque required to twist a pair of extensible filaments that can be modeled as a neo-Hookean material. Geometry is shown to play an important role in determining the torque required to twist the filament pair. By performing torque measurements and calculating them using an energy based approach, we have developed a deeper understanding of how energy is distributed in a twisted filament pair. We find that a surprisingly large amount of energy is stored in stretching. In fact, it is typically greater than in the twisting component for sufficiently large separation distances or pre-stretching.

The overall torque profile, namely the rapid initial increase and peak, and then a slower increase is a feature of the geometry of the system. These features are

true not only for nonlinear neo-Hookean materials, but for Hookean materials as well. We provide analytical formulas in the Hookean limit which can prove useful in calculating the energy in twisted filaments which are increasingly being considered in energy storage applications. These formulas can be inverted to obtain the twist angles reached for a given applied torque and initial twist angle. Further, our results further invite critical examination of analysis of twisted polymeric systems which focus on bending while considering the elastic energy stored in the system, and neglect stretching [21, 23].

Acknowledgements

This work was supported under U.S. National Science Foundation grant DMR-2005090.

-
- [1] J. Bohr and K. Olsen. The ancient art of laying rope. *EPL (Europhysics Letters)*, 93(6):60004, March 2011.
- [2] Antoine Legrain, Erwin JW Berenschot, Leon Abelmann, José Bico, and Niels R Tas. Let’s twist again: elasto-capillary assembly of parallel ribbons. *Soft matter*, 12(34):7186–7194, 2016.
- [3] Nicholas Weiner, Yashraj Bhosale, Mattia Gazzola, and Hunter King. Mechanics of randomly packed filaments—the “bird nest” as meta-material. *Journal of Applied Physics*, 127(5), 2020.
- [4] Valentin M. Slepukhin, Maximilian J. Grill, Qingda Hu, Elliot L. Botvinick, Wolfgang A. Wall, and Alex J. Levine. Topological defects produce kinks in biopolymer filament bundles. *Proceedings of the National Academy of Sciences*, 118(15):e2024362118, 2021.
- [5] Xiang Gao, Yifeng Hong, Fan Ye, James T. Inman, and Michelle D. Wang. Torsional stiffness of extended and plectonemic dna. *Phys. Rev. Lett.*, 127:028101, Jul 2021.
- [6] Thomas B. Plumb-Reyes, Nicholas Charles, and L. Mahadevan. Combing a double helix. *Soft Matter*, 18:2767–2775, 2022.
- [7] Antoine Seguin and Jérôme Crassous. Twist-controlled force amplification and spinning tension transition in yarn. *Physical Review Letters*, 128(7):078002, 2022.
- [8] Vishal P. Patil, Harry Tuazon, Emily Kaufman, Tuhin Chakraborty, David Qin, Jörn Dunkel, and M. Saad Bhamla. Ultrafast reversible self-assembly of living tangled matter. *Science*, 380(6643):392–398, 2023.
- [9] Paul Grandgeorge, Changyeob Baek, Harmeet Singh, Paul Johanns, Tomohiko G. Sano, Alastair Flynn, John H. Maddocks, and Pedro M. Reis. Mechanics of two filaments in tight orthogonal contact. *Proceedings of the National Academy of Sciences*, 118(15):e2021684118, 2021.
- [10] Moshe Shoham. Twisting Wire Actuator. *Journal of Mechanical Design*, 127(3):441–445, 07 2004.
- [11] James J. Guzek, Conrad Petersen, Stephane Constantin, and Hod Lipson. Mini Twist: A Study of Long-Range Linear Drive by String Twisting. *Journal of Mechanisms and Robotics*, 4(1), 02 2012. 014501.
- [12] C. H. Kwon, S. H. Lee, Y.-B. Choi, J. A. Lee, S. H. Kim, H. H. Kim, G. M. Spinks, G. G. Wallace, M. D. Lima, M. E. Kozlov, R. H. Baughman, and S. J. Kim. High-power biofuel cell textiles from woven bisrolled carbon nanotube yarns. *Nat. Commun.*, 5(1):1–7, 2014.
- [13] Carter S. Haines, Na Li, Geoffrey M. Spinks, Ali E. Aliev, Jiangtao Di, and Ray H. Baughman. New twist on artificial muscles. *Proceedings of the National Academy of Sciences*, 113:11709 – 11716, 2016.
- [14] Nicholas Charles, Mattia Gazzola, and L Mahadevan. Topology, geometry, and mechanics of strongly stretched and twisted filaments: solenoids, plectonemes, and artificial muscle fibers. *Physical review letters*, 123(20):208003, 2019.
- [15] John Thompson and A. Champneys. From helix to localized writhing in the torsional post-buckling of elastic rods. *Proceedings: Mathematical, Physical and Engineering Sciences*, 452:The Royal Society–, 01 1996.
- [16] Basile Audoly. *CHAPTER 1: Introduction to the elasticity of rods*, pages 1–24. 01 2016.
- [17] Kasper Olsen and Jakob Bohr. Geometry of the toroidal n-helix: optimal-packing and zero-twist. *New Journal of Physics*, 14(2):023063, feb 2012.
- [18] Gregory M. Grason. Colloquium: Geometry and optimal packing of twisted columns and filaments. *Rev. Mod. Phys.*, 87:401–419, May 2015.
- [19] S. Neukirch and G. van der Heijden. Geometry and mechanics of uniform n-ply: From engineering ropes to biological filaments. *Journal of Elasticity*, 69:41–72, 11 2002.
- [20] Gregory M. Grason. Defects in crystalline packings of twisted filament bundles. i. continuum theory of disclinations. *Phys. Rev. E*, 85:031603, Mar 2012.
- [21] Andreea Panaitescu, Gregory M. Grason, and Arshad Kudrolli. Persistence of perfect packing in twisted bundles of elastic filaments. *Phys. Rev. Lett.*, 120:248002, Jun 2018.
- [22] Jesse M. Hanlan, Gabrielle E. Davis, and Douglas J. Durian. Twist and measure: characterizing the effective radius of strings and bundles under twisting contraction. *Soft Matter*, 19:4315–4322, 2023.
- [23] Gilles Charvin, Alexander Vologodskii, David Bensimon,

- and Vincent Croquette. Braiding dna: Experiments, simulations, and models. *Biophysical Journal*, 88:4124–36, 07 2005.
- [24] Isaac R. Bruss and Gregory M. Grason. Topological defects, surface geometry and cohesive energy of twisted filament bundles. *Soft Matter*, 9:8327–8345, 2013.
- [25] Julien Chopin and Arshad Kudrolli. Tensional twist-folding of sheets into multilayered scrolled yarns. *Science Advances*, 8(14), apr 2022.
- [26] Basile Audoly and Yves Pomeau. *Elasticity and Geometry*. Oxford University Press, New York, 2010.
- [27] Ray W. Ogden. *Non-Linear Elastic Deformations*. Dover, New York, 1984.
- [28] Barrett O’neill. *Elementary differential geometry*. Elsevier, 2006.
- [29] Ronald S. Rivlin and D.W. Saunders. Large elastic deformations of isotropic materials vii. experiments on the deformation of rubber. *Philosophical Transactions of the Royal Society of London. Series A, Mathematical and Physical Sciences*, 243(865):251–288, 1951.
- [30] R.S. Rivlin. Large elastic deformations of isotropic materials. iii. some simple problems in cylindrical polar coordinates. *Philosophical Transactions of the Royal Society of London. Series A, Mathematical and Physical Sciences*, 240(823):509–525, 1948.
- [31] A. Ghatak and L. Mahadevan. Solenoids and plectonemes in stretched and twisted elastomeric filaments. *Phys. Rev. Lett.*, 95:057801, Jul 2005.
- [32] Kenneth Langstreth Johnson. *Contact mechanics*. Cambridge university press, 1987.